

Resolution of $B \rightarrow (J/\Psi, \eta_c)K$ puzzle in the perturbative QCD approach

Xin Liu*, Zhi-Qing Zhang[†] and Zhen-Jun Xiao[‡]

*Department of Physics and Institute of Theoretical Physics,
Nanjing Normal University, Nanjing, Jiangsu 210097, P.R. China*
(Dated: February 6, 2020)

Abstract

In this paper, we calculate the $B \rightarrow (J/\Psi, \eta_c)K$ decays in the perturbative QCD approach with the inclusion of the important next-to-leading order (NLO) contributions. We find numerically that (a) the NLO pQCD predictions for the branching ratios are: $Br(B^0 \rightarrow J/\Psi K^0) = 9.9_{-3.2}^{+4.0} \times 10^{-4}$, $Br(B^+ \rightarrow J/\Psi K^+) = 10.6_{-3.3}^{+4.3} \times 10^{-4}$, $Br(B^0 \rightarrow \eta_c K^0) = 7.0_{-2.0}^{+2.3} \times 10^{-4}$, $Br(B^+ \rightarrow \eta_c K^+) = 7.5_{-2.2}^{+2.7} \times 10^{-4}$, which agree very well with the data, and therefore the so-called “ $B \rightarrow (J/\Psi, \eta_c)K$ ” puzzle is resolved by the inclusion of the NLO vertex corrections; (b) the NLO pQCD predictions for the CP-violating asymmetries of $B \rightarrow (J/\Psi, \eta_c)K$ decays also agree perfectly with the data.

PACS numbers: 13.25.Hw, 12.38.Bx, 14.40.Nd

arXiv:0901.0165v1 [hep-ph] 1 Jan 2009

* hsinlau@126.com

† zhangzhiqing@zzu.edu.cn

‡ xiaozhenjun@njnu.edu.cn

I. INTRODUCTION

The $B \rightarrow J/\Psi K$ and $B \rightarrow \eta_c K$ decays are phenomenologically very interesting decay modes and have drawn a great attention for many years. Although the underlying weak decay of $b \rightarrow c\bar{c}s$ is simple, but a clear understanding of the exclusive $B \rightarrow (J/\Psi, \eta_c)K$ decays is really difficult because of the involving of the complex strong-interaction effects.

On the experiments side, the experimental studies for the "Golden-plated" $B \rightarrow J/\Psi K_{S,L}$ decays result in the precision measurement of $\sin 2\beta$ [1]. The branching ratios of $B \rightarrow (J/\Psi, \eta_c)K$ decays and other similar decays involving a charmonium and a light pseudo-scalar or vector meson as the two final state meson, have been measured with good or high precision [1, 2]:

$$\begin{aligned} Br(B^0 \rightarrow J/\Psi K^0) &= (8.71 \pm 0.32) \times 10^{-4}, \\ Br(B^+ \rightarrow J/\Psi K^+) &= (10.07 \pm 0.35) \times 10^{-4}, \end{aligned} \quad (1)$$

$$\begin{aligned} Br(B^0 \rightarrow \eta_c K^0) &= (8.9 \pm 1.6) \times 10^{-4}, \\ Br(B^+ \rightarrow \eta_c K^+) &= (9.1 \pm 1.3) \times 10^{-4}. \end{aligned} \quad (2)$$

The accuracy of above measurements will be improved rapidly along with the running of the relevant LHC experiments.

On the theory side, such B meson charmonia decays have been studied intensively by employing various theoretical methods or approaches, for example, in Refs. [3, 4, 5, 6, 7, 8, 9, 10, 11, 12, 13]. But unfortunately, it is still very difficult to give an explanation for the corresponding data without the worry about the serious problems.

For $B \rightarrow J/\Psi K$ decay, for example, the theoretical predictions for its branching ratio in both the naive factorization approach (NFA) [4] and the QCD factorization (QCDF) approach[14] are much smaller (a factor of $7 \sim 10$) than the measured values[5]: $Br(B \rightarrow J/\Psi K) \sim 1.1 \times 10^{-4}$ when the twist-2 distribution function (DA) $\phi_\psi(x) = 6x(1-x)$ was employed [5].

In Ref. [6], the authors studied the effects of twist-3 DA ϕ_σ^K and found that the resultant enhancement to the Wilson coefficient $a_2(J/\Psi K)$ and consequently to the branching ratio $Br(b \rightarrow J/\Psi K)$, induced through the spectator diagram, can be large. But one should note that there are also logarithmic divergences arising from spectator interactions due to kaon twist-3 effects, this is always a serious problem in the QCDF approach.

In Refs. [8, 9], the authors studied the decays $B \rightarrow (\eta_c, \eta'_c, \chi_{cJ})K$ in the QCDF approach and found that (a) the logarithmic divergences will arise from the spectator interactions due to the kaon twist-3 effects; and (b) the predicted decay rate is $Br(B \rightarrow \eta_c K) = 1.9 \times 10^{-4}$, which is too small by a factor of 5 compared to the measured value as given in Eq.(2). They concluded that the QCDF approach with its present version can not be safely applied to exclusive decays of B meson into charmonia [9].

The $B \rightarrow J/\Psi K$ decays have also been investigated by employing the QCD Light-cone sum rules (LCSR) [10]. The authors calculated the nonfactorizable contributions to the $B \rightarrow J/\Psi K$ decay coming from the exchanges of the soft gluons between the emitted J/Ψ and the kaon. But their predictions for branching ratios is still too small, $Br(B \rightarrow J/\Psi K) \sim 3.3 \times 10^{-4}$, to accommodate the data.

In Refs.[12, 13], the authors studied $B \rightarrow (J/\Psi, \eta_c, \chi_{c0,c1})K^{(*)}$ decays in a formalism that combines the QCDF factorization and the perturbive QCD (pQCD) approaches[11]. They employed the QCDF approach to calculate the factorizable contribution, but the

pQCD approach to evaluate the nonfactorizable corrections to the considered decays. According to their studies[12, 13] we see that (a) the theoretical predictions for the branching ratios of $B \rightarrow (J/\Psi, \chi_{c0,c1})K$ decays can be large and consistent with the data; (b) the $B \rightarrow \eta_c K$ decays still exhibit a puzzle: the predicted result is $Br(B \rightarrow \eta_c K) \approx 2.3 \times 10^{-4}$, much smaller than the measured values as given in Eq. (1). Furthermore, it should be mentioned that these results[12, 13] were obtained by treating one decay with two different factorization approaches: the self-consistency of such “mixing-approach” may be a serious problem.

Up to now, a clear and satisfactory theoretical interpretation for the measured large decay rates of $B \rightarrow (J/\Psi, \eta_c)K$ are still absent. We call this situation the “ $B \rightarrow (J/\Psi, \eta_c)K$ ” puzzle. In this paper, we will calculate the branching ratios and CP-violating asymmetries of the four $B \rightarrow (J/\Psi, \eta_c)K$ decays by employing the pQCD factorization approach: (a) we evaluate both the factorizable and nonfactorizable contributions in the pQCD approach; (b) besides the full leading order (LO) contributions in the pQCD approach, the currently known next-to-leading order (NLO) contributions [15] (specifically the QCD vertex corrections for the considered decays) are also included; and (c) we found that the QCD vertex corrections play the key role to resolve the “ $B \rightarrow (J/\Psi, \eta_c)K$ ” puzzle.

The paper is organized as follows: in Sec. II, we firstly present the formalism of the pQCD approach, and then make the analytic calculations and show the decay amplitudes for the considered decays. In Sec. III, we show the numerical results and compare them with the measured values. A short summary and some conclusions are given in the last section.

II. FORMALISM AND PERTURBATIVE CALCULATIONS

A. Formalism

In recent years, the pQCD factorization approach has been used frequently to calculate various B meson decay channels. For the two body charmless hadronic B meson decays the pQCD predictions for the branching ratios and CP-violating asymmetries generally agree well with the measured values [16, 17, 18, 19, 20, 21]. In Ref. [22], the authors calculated $B \rightarrow D_s^* K, D_s^{(*)+} D_s^{(*)-}$ and $B_s \rightarrow D^{(*)+} D^{(*)-}$ decays and found that the pQCD approach works well for such decays. In a previous paper[23], the $B \rightarrow J/\Psi K$ decays have been studied by employing the pQCD approach at leading order. Here we try to apply the pQCD approach to calculate the $B \rightarrow (J/\Psi, \eta_c)K$ decays with the inclusion of the NLO corrections.

In pQCD approach, the decay amplitude of $B \rightarrow M_2 M_3$ decays¹ can be written conceptually as the convolution,

$$\mathcal{A}(B \rightarrow M_2 M_3) \sim \int d^4 k_1 d^4 k_2 d^4 k_3 \text{Tr} [C(t) \Phi_B(k_1) \Phi_{M_2}(k_2) \Phi_{M_3}(k_3) H(k_1, k_2, k_3, t)], \quad (3)$$

where the term “Tr” denotes the trace over Dirac and color indices. $C(t)$ is the Wilson coefficient which results from the radiative corrections at short distance. In the above

¹ Here $M_2 = (J/\Psi, \eta_c)$ is the emitted charmonium, and M_3 is the kaon which absorbed the spectator quark.

convolution, $C(t)$ includes the harder dynamics at larger scale than m_B scale and describes the evolution of local 4-Fermi operators from m_W (the W boson mass) down to $t \sim \mathcal{O}(\sqrt{\bar{\Lambda}m_B})$ scale, where $\bar{\Lambda} \equiv m_B - m_b$. The function $H(k_1, k_2, k_3, t)$ is the hard part and can be calculated perturbatively. The function Φ_M is the wave function which describes hadronization of the quark and anti-quark to the meson M . While the function H depends on the process considered, the wave function Φ_M is independent of the specific process. Using the wave functions determined from other well measured processes, one can make quantitative predictions here.

Using the light-cone coordinates the B meson and the two final state meson momenta can be written as

$$P_1 = \frac{m_B}{\sqrt{2}}(1, 1, \mathbf{0}_T), \quad P_2 = \frac{m_B}{\sqrt{2}}(1, r^2, \mathbf{0}_T), \quad P_3 = \frac{m_B}{\sqrt{2}}(0, 1 - r^2, \mathbf{0}_T), \quad (4)$$

respectively, where $r = m_{M_2}/m_B$, and the light pseudo-scalar meson masses $m_{M_3} = m_K$ have been neglected. The longitudinal polarization of vector J/Ψ , ϵ_L , is given by $\epsilon_L = \frac{m_B}{\sqrt{2}m_{J/\Psi}}(1, -r_{J/\Psi}^2, \mathbf{0}_T)$. Putting the light (anti-) quark momenta in B , M_2 and M_3 mesons as k_1 , k_2 , and k_3 , respectively, we can choose

$$k_1 = (x_1 P_1^+, 0, \mathbf{k}_{1T}), \quad k_2 = (x_2 P_2^+, 0, \mathbf{k}_{2T}), \quad k_3 = (0, x_3 P_3^-, \mathbf{k}_{3T}). \quad (5)$$

Then, the integration over k_1^- , k_2^- , and k_3^+ in Eq.(3) will lead to

$$\mathcal{A}(B \rightarrow M_2 M_3) \sim \int dx_1 dx_2 dx_3 b_1 db_1 b_2 db_2 b_3 db_3 \cdot \text{Tr} [C(t) \Phi_B(x_1, b_1) \Phi_{M_2}(x_2, b_2) \Phi_{M_3}(x_3, b_3) H(x_i, b_i, t) S_t(x_i) e^{-S(t)}] \quad (6)$$

where b_i is the conjugate space coordinate of k_{iT} , and t is the largest energy scale in function $H(x_i, b_i, t)$. The large logarithms $\ln(m_W/t)$ are included in the Wilson coefficients $C(t)$. The large double logarithms ($\ln^2 x_i$) on the longitudinal direction are summed by the threshold resummation [24], and they lead to $S_t(x_i)$ which smears the end-point singularities on x_i . The last term, $e^{-S(t)}$, is the Sudakov form factor which suppresses the soft dynamics effectively [25]. Thus it makes the perturbative calculation of the hard part H applicable at intermediate scale, i.e., m_B scale.

For the considered decays, the weak effective Hamiltonian \mathcal{H}_{eff} for $b \rightarrow s$ transition can be written as

$$\mathcal{H}_{eff} = \frac{G_F}{\sqrt{2}} \left[V_{cb}^* V_{cs} (C_1(\mu) O_1^c(\mu) + C_2(\mu) O_2^c(\mu)) - V_{tb}^* V_{ts} \sum_{i=3}^{10} C_i(\mu) O_i(\mu) \right], \quad (7)$$

where $C_i(\mu)$ are Wilson coefficients at the renormalization scale μ and O_i are the four-fermion operators:

$$\begin{aligned} O_1^c &= \bar{s}_\alpha \gamma^\mu L c_\beta \cdot \bar{c}_\beta \gamma_\mu L b_\alpha, & O_2^c &= \bar{s}_\alpha \gamma^\mu L c_\alpha \cdot \bar{c}_\beta \gamma_\mu L b_\beta, \\ O_3 &= \bar{s}_\alpha \gamma^\mu L b_\alpha \cdot \sum_{q'} \bar{q}'_\beta \gamma_\mu L q'_\beta, & O_4 &= \bar{s}_\alpha \gamma^\mu L b_\beta \cdot \sum_{q'} \bar{q}'_\beta \gamma_\mu L q'_\alpha, \\ O_5 &= \bar{s}_\alpha \gamma^\mu L b_\alpha \cdot \sum_{q'} \bar{q}'_\beta \gamma_\mu R q'_\beta, & O_6 &= \bar{s}_\alpha \gamma^\mu L b_\beta \cdot \sum_{q'} \bar{q}'_\beta \gamma_\mu R q'_\alpha, \\ O_7 &= \frac{3}{2} \bar{s}_\alpha \gamma^\mu L b_\alpha \cdot \sum_{q'} e_{q'} \bar{q}'_\beta \gamma_\mu R q'_\beta, & O_8 &= \frac{3}{2} \bar{s}_\alpha \gamma^\mu L b_\beta \cdot \sum_{q'} e_{q'} \bar{q}'_\beta \gamma_\mu R q'_\alpha, \\ O_9 &= \frac{3}{2} \bar{s}_\alpha \gamma^\mu L b_\alpha \cdot \sum_{q'} e_{q'} \bar{q}'_\beta \gamma_\mu L q'_\beta, & O_{10} &= \frac{3}{2} \bar{s}_\alpha \gamma^\mu L b_\beta \cdot \sum_{q'} e_{q'} \bar{q}'_\beta \gamma_\mu L q'_\alpha, \end{aligned} \quad (8)$$

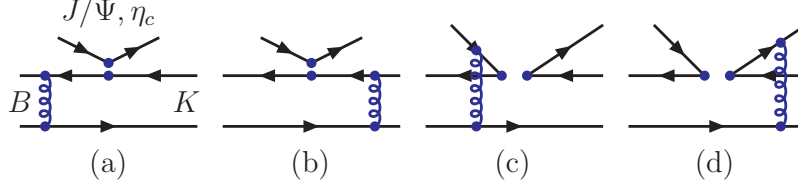


FIG. 1: Typical Feynman diagrams contributing to $B \rightarrow (J/\Psi, \eta_c)K$ and $B_s \rightarrow (J/\Psi, \eta_c)\bar{K}^0$ decays at leading order.

where α and β are the $SU(3)$ color indices; L and R are the left- and right-handed projection operators with $L = (1 - \gamma_5)$, $R = (1 + \gamma_5)$. The sum over q' runs over the quark fields that are active at the scale $\mu = O(m_b)$, i.e., $q' \in \{u, d, s, c, b\}$. For the case of $b \rightarrow d$ transition, simply makes a replacement of s by d in Eq. (7) and in the expressions of O_i operators.

In PQCD approach, the scale “ t ” appeared in the Wilson coefficients $C_i(t)$, the hard-kernel $H(x_i, b_i, t)$ and the Sudakov factor $e^{-S(t)}$ is chosen as the largest energy scale in the gluon and/or the quark propagators of a given Feynman diagram, in order to suppress the higher order corrections and improve the reliability of the perturbative calculation. Here, the scale “ t ” may be larger or smaller than the m_b scale. In the range of $t < m_b$ or $t \geq m_b$, the number of active quarks is $N_f = 4$ or $N_f = 5$, respectively. For the Wilson coefficients $C_i(\mu)$ and their renormalization group (RG) running, they are known at NLO level currently [26]. The explicit expressions of the LO and NLO $C_i(m_{B_s})$ can be found easily, for example, in Refs. [26, 27].

When the pQCD approach at leading-order are employed, the leading order Wilson coefficients $C_i(m_W)$, the leading order RG evolution matrix $U(t, m)^{(0)}$ from the high scale m down to $t < m$ and the leading order $\alpha_s(t)$ are used:

$$\alpha_s(t) = \frac{4\pi}{\beta_0 \ln [t^2/\Lambda_{QCD}^2]}, \quad (9)$$

where $\beta_0 = (33 - 2N_f)/3$.

When the NLO contributions are taken into account, however, the NLO Wilson coefficients $C_i(m_W)$, the NLO RG evolution matrix $U(t, m, \alpha)$ (see Eq. (7.22) in Ref. [26]) and the $\alpha_s(t)$ at two-loop level will be used:

$$\alpha_s(t) = \frac{4\pi}{\beta_0 \ln [t^2/\Lambda_{QCD}^2]} \cdot \left\{ 1 - \frac{\beta_1}{\beta_0^2} \cdot \frac{\ln [\ln [t^2/\Lambda_{QCD}^2]]}{\ln [t^2/\Lambda_{QCD}^2]} \right\}, \quad (10)$$

where $\beta_0 = (33 - 2N_f)/3$, $\beta_1 = (306 - 38N_f)/3$. By assuming $\Lambda_{QCD}^{(5)} = 0.225$ GeV, we will get $\Lambda_{QCD}^{(4)} = 0.287$ GeV (0.326 GeV) for LO (NLO) case.

As discussed in Ref.[20], it is reasonable to choose $\mu_0 = 1.0$ GeV as the lower cut-off of the hard scale t . In the numerical integrations we will fix the values $C_i(t)$ at $C_i(1.0)$ whenever the scale t runs below the scale $\mu_0 = 1.0$ GeV [20, 21], unless otherwise stated. We will also consider the effects of varying the μ_0 in the region of $1 \leq \mu_0 \leq 2$ GeV in the next section.

B. $B \rightarrow J/\Psi M_3$ decays at leading order

At the leading order pQCD approach, as illustrated in Fig. 1, the relevant Feynman diagrams for the considered decays include the factorizable emission diagrams (Figs.1a and 1b) and the non-factorizable spectator ones (Figs.1c and 1d). The operators $O_{1,2}$, $O_{3,4}$ and $O_{9,10}$ are the $(V - A)(V - A)$ currents, while $O_{4,5}$ and $O_{7,8}$ are the $(V - A)(V + A)$ currents. By analytic calculations of Fig.1a and 1b, one finds the corresponding decay amplitudes

$$\begin{aligned}
F_{J/\Psi M_3}^{V-A} &= 8\pi C_F m_B^2 \int_0^1 dx_1 dx_3 \int_0^\infty b_1 db_1 b_3 db_3 \phi_B(x_1, b_1) \\
&\times \left\{ \left[[(1-r^2)(1+x_3) - x_3 r^2] \phi_{M_3}^A(x_3) + r_0(1-2x_3) [\phi_{M_3}^P(x_3) + \phi_{M_3}^T(x_3)] \right. \right. \\
&\quad \left. \left. - r_0 r^2 [(1-2x_3)\phi_{M_3}^P(x_3) - (1+2x_3)\phi_{M_3}^T(x_3)] \right] \right. \\
&\quad \cdot \alpha_s(t_e^1) h_e(x_1, x_3, b_1, b_3) \exp[-S_{ab}(t_e^1)] \\
&\quad \left. + 2r_0(1-r^2) \phi_{M_3}^P(x_3) \cdot \alpha_s(t_e^2) h_e(x_3, x_1, b_3, b_1) \exp[-S_{ab}(t_e^2)] \right\}, \quad (11)
\end{aligned}$$

where $r_0 = m_0^K/m_B$, and $C_F = 4/3$ is a color factor. The hard function h_e , the scales t_e^i and the Sudakov factors S_{ab} are displayed in Appendix A.

Now we consider the contributions of the operators $O_{5,6,7,8}$ in the Fig.1. In some decay channels, some of these operators contribute to the decay amplitude in a factorizable way. Since only the vector part of $(V + A)$ current contribute to the vector meson production, $\langle M_3 | V - A | B \rangle \langle J/\Psi | V + A | 0 \rangle = \langle M_3 | V - A | B \rangle \langle J/\Psi | V - A | 0 \rangle$, that is

$$F_{J/\Psi M_3}^{V+A} = F_{J/\Psi M_3}^{V-A}. \quad (12)$$

For the non-factorizable diagrams 1(c) and 1(d), all three meson wave functions are involved. The integration of b_3 can be performed using δ function $\delta(b_3 - b_1)$, leaving only integration of b_1 and b_2 . For the $(V - A)(V - A)$ operators, the corresponding decay amplitude is

$$\begin{aligned}
M_{J/\Psi M_3}^{V-A} &= -\frac{16\sqrt{6}}{3} \pi C_F m_B^2 \int_0^1 dx_1 dx_2 dx_3 \int_0^\infty b_1 db_1 b_2 db_2 \phi_B(x_1, b_1) \\
&\times \left\{ 2rr_c \phi_{J/\Psi}^t(x_2) \phi_{M_3}^A(x_3) - 4rr_0 r_c \phi_{J/\Psi}^t(x_2) \phi_{M_3}^T(x_3) \right. \\
&\quad \left. - [x_3 + 2(x_2 - x_3)r^2] \phi_{J/\Psi}^L(x_2) \phi_{M_3}^A(x_3) \right. \\
&\quad \left. + 2r_0 [x_3 + (2x_2 - x_3)r^2] \phi_{J/\Psi}^L(x_2) \phi_{M_3}^T(x_3) \right\} \\
&\quad \cdot \alpha_s(t_f) h_f(x_1, x_2, x_3, b_1, b_2) \exp[-S_{cd}(t_f)]. \quad (13)
\end{aligned}$$

where $r_c = m_c/m_B$ and m_c is the mass for c quark.

For some decay channels, the $(S - P)(S + P)$ operators can be obtained from the $(V - A)(V + A)$ operators by making the Fierz transformation, in order to get right color

and flavor structure for factorization to work. For these $(S - P)(S + P)$ operators, the corresponding decay amplitude can be written as

$$M_{J/\Psi M_3}^{S+P} = -M_{J/\Psi M_3}^{V-A}. \quad (14)$$

For $B \rightarrow J/\Psi M_3$ decays, by combining the contributions from different Feynman diagrams, the total decay amplitude can be written as

$$\begin{aligned} \mathcal{M}(B \rightarrow J/\Psi M_3) &= F_{J/\Psi M_3}^{V-A} f_{J/\Psi} \{V_{cb}^* V_{cs} a_2 - V_{tb}^* V_{ts} (a_3 + a_5 + a_7 + a_9)\} \\ &+ M_{J/\Psi M_3}^{V-A} \{V_{cb}^* V_{cs} C_2 - V_{tb}^* V_{ts} (C_4 - C_6 - C_8 + C_{10})\}, \end{aligned} \quad (15)$$

where a_i is the combination of the Wilson coefficients C_i :

$$a_2 = C_1 + \frac{C_2}{3}; \quad a_i = C_i + \frac{C_{i+1}}{3}, \quad \text{for } i = 3, 5, 7, 9, \quad (16)$$

where $C_2 \sim 1$ is the largest one among all Wilson coefficients.

C. $B \rightarrow \eta_c M_3$ decays at leading order

Following the same procedure as for $B \rightarrow J/\Psi K$ decays, it is straightforward to calculate the decay amplitudes for $B \rightarrow \eta_c M_3$ decays.

$$\begin{aligned} \mathcal{M}(B \rightarrow \eta_c M_3) &= F_{\eta_c M_3}^{V-A} f_{\eta_c} [V_{cb}^* V_{cs} a_2 - V_{tb}^* V_{ts} (a_3 + a_5 + a_7 + a_9)] \\ &+ M_{\eta_c M_3}^{V-A} [V_{cb}^* V_{cs} C_2 - V_{tb}^* V_{ts} (C_4 + C_6 + C_8 + C_{10})], \end{aligned} \quad (17)$$

where the functions $F_{\eta_c M_3}^{V-A}$, $M_{\eta_c M_3}^{V-A}$, etc, are of the form

$$\begin{aligned} F_{\eta_c M_3}^{V-A} &= -F_{\eta_c M_3}^{V+A} = 8\pi C_F m_B^2 \int_0^1 dx_1 dx_3 \int_0^\infty b_1 db_1 b_3 db_3 \phi_B(x_1, b_1) \\ &\times \left\{ \left[[(1-r^2)(1+x_3) - x_3 r^2] \phi_{M_3}^A(x_3) + r_0(1-2x_3) [\phi_{M_3}^P(x_3) + \phi_{M_3}^T(x_3)] \right. \right. \\ &\left. \left. + r_0 r^2 [(1+2x_3)\phi_{M_3}^P(x_3) - (1-2x_3)\phi_{M_3}^T(x_3)] \right] \right. \\ &\left. \cdot \alpha_s(t_e^1) h_e(x_1, x_3, b_1, b_3) \exp[-S_{ab}(t_e^1)] \right. \\ &\left. + 2r_0(1-r^2) \phi_{M_3}^P(x_3) \cdot \alpha_s(t_e^2) h_e(x_3, x_1, b_3, b_1) \exp[-S_{ab}(t_e^2)] \right\}, \end{aligned} \quad (18)$$

$$\begin{aligned} M_{\eta_c M_3}^{V-A} &= M_{\eta_c M_3}^{S+P} = -\frac{16\sqrt{6}}{3} \pi C_F m_B^2 \int_0^1 dx_1 dx_2 dx_3 \int_0^\infty b_1 db_1 b_2 db_2 \phi_B(x_1, b_1) \phi_{\eta_c}^v(x_2, b_2) \\ &\times x_3 \left[(1-2r^2) \phi_{M_3}^A(x_3) - 2r_0(1-r^2) \phi_{M_3}^T(x_3) \right] \\ &\cdot \alpha_s(t_f) h_f(x_1, x_2, x_3, b_1, b_2) \exp[-S_{cd}(t_f)], \end{aligned} \quad (19)$$

where $\phi_{\eta_c}^v$ is the leading twist-2 part of the distribution amplitude for the pseudo-scalar meson η_c .

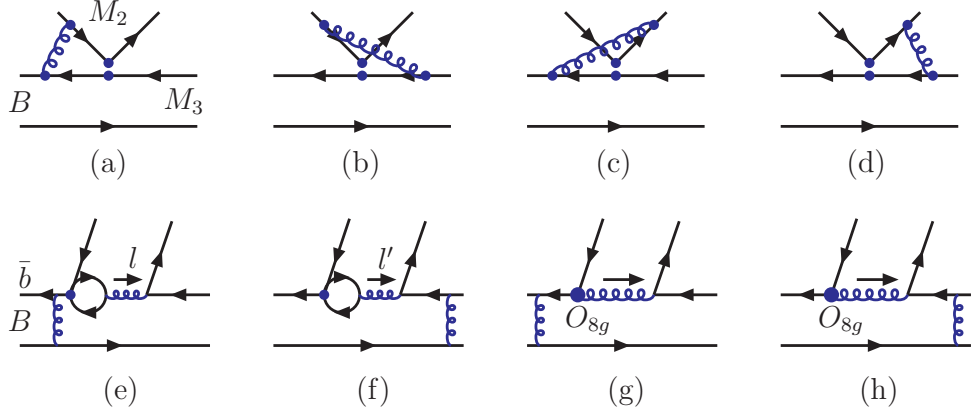


FIG. 2: Typical Feynman diagrams contributing to $B \rightarrow M_2 M_3$ decays at NLO level.

D. NLO contributions in pQCD approach

For a general $B \rightarrow M_2 M_3$ decays, the power counting in the pQCD factorization approach [15] is different from that in the QCD factorization [14]. In the pQCD approach, the NLO contributions may include the following parts [15, 20]:

1. The Wilson coefficients $C_i(m_{B_s})$ and the renormalization group evolution matrix $U(t, m, \alpha)$ at NLO level, and the $\alpha_s(t)$ at two-loop level [26] should be used.
2. All the Feynman diagrams, which lead to the decay amplitudes proportional to $\alpha_s^2(t)$, should be considered.
3. Currently known NLO contributions: (a) the vertex corrections; (b) the contributions from the quark-loops and the chromo-magnetic penguins (O_{8g}), as illustrated in Fig. 2.
4. The NLO contributions can also come from the Feynman diagrams as shown in the Figs. 5-7 in Ref. [20]. The analytical calculations for these (more than 100!) Feynman diagrams have not been completed yet.

For the considered $B \rightarrow J/\Psi K$ and $\eta_c K$ decays, only the vertex corrections (see Fig.2a-2d) among the known NLO contributions will contribute. For the four vertex correction diagrams Fig.2a-2d, as was confirmed in Ref.[6], the infrared divergences from the soft gluons and collinear gluons in the four diagrams will be canceled each other, respectively. So the total contributions of these four figures are infrared finite. In other words, these vertex corrections can be calculated without considering the transverse momentum effects of the quark at the end-point region in collinear factorization theorem. Therefore, there is no need to employ the k_T factorization theorem here. The vertex corrections to the $B \rightarrow J/\psi K$ decays, denoted as f_I in QCDF, have been calculated in the NDR scheme [5, 6], and can be adopted directly. Their effects can be combined into the Wilson coefficients

associated with the factorizable contributions:

$$a_2 = C_1 + \frac{C_2}{N_c} + \frac{\alpha_s C_F}{4\pi N_c} C_2 \left(-18 + 12 \ln \frac{m_b}{\mu} + f_I \right), \quad (20)$$

$$a_3 = C_3 + \frac{C_4}{N_c} + \frac{\alpha_s C_F}{4\pi N_c} C_4 \left(-18 + 12 \ln \frac{m_b}{\mu} + f_I \right),$$

$$a_5 = C_5 + \frac{C_6}{N_c} + \frac{\alpha_s C_F}{4\pi N_c} C_6 \left(6 - 12 \ln \frac{m_b}{\mu} - f_I \right), \quad (21)$$

$$a_7 = C_7 + \frac{C_8}{N_c} + \frac{\alpha_s C_F}{4\pi N_c} C_8 \left(6 - 12 \ln \frac{m_b}{\mu} - f_I \right),$$

$$a_9 = C_9 + \frac{C_{10}}{N_c} + \frac{\alpha_s C_F}{4\pi N_c} C_{10} \left(-18 + 12 \ln \frac{m_b}{\mu} + f_I \right). \quad (22)$$

with the function f_I ,

$$f_I = \frac{2\sqrt{2N_c}}{f_{J/\psi}} \int dx_2 \Psi^L(x_2) \left[\frac{3(1-2x_2)}{1-x_2} \ln x_2 - 3\pi i + 3 \ln(1-r_2^2) + \frac{2r_2^2(1-x_2)}{1-r_2^2 x_2} \right], \quad (23)$$

where $r_2 = m_{J/\Psi}/m_B$ and those terms proportional to r_2^4 have been neglected. In Eqs.(20-22), the Wilson coefficients C_i at NLO level should be used when the NLO vertex corrections are taken into account.

For $B \rightarrow \eta_c K$ decays, it is easy to obtain the corresponding NLO vertex corrections from those Wilson coefficients in Eqs. (20-22), by the replacement of the parameter $f_{J/\Psi}$ and $r_2(J/\Psi)$ in f_I with f_{η_c} and $r_2(\eta_c)$ [9], respectively.

Since both $B \rightarrow J/\Psi K$ and $\eta_c K$ are color-suppressed decays, the Wilson coefficient a_2 in general plays the dominate role. It is instructive to check the variation of a_2 at LO or NLO level, with or without the inclusion of the NLO vertex corrections. In Figs.3a and 3b, the solid (dashed) curve stands for a_2 at NLO (LO) level without the vertex corrections, while the dotted (dash-dotted) curve refers to the real (imaginary) part of the a_2 at NLO level with the vertex corrections. From Figs.3a and 3b, one can see that (a) the μ -dependence of $a_2(J/\Psi K)$ and $a_2(\eta_c K)$ are very similar; (b) the μ -dependence of a_2 is decreased effectively due to the inclusion of the NLO vertex corrections; and (c) the vertex correction provides a large imaginary part to a_2 , and therefore an effective enhancement of $|a_2|$ due to the vertex correction is expected.

III. NUMERICAL RESULTS AND DISCUSSIONS

A. Branching ratios

The input parameters and the wave functions to be used in the numerical calculations are given in Appendix B.

Firstly, we find the pQCD predictions for the corresponding form factors at zero momentum transfer:

$$F_0^{B \rightarrow K}(q^2 = 0) = 0.32_{-0.05}^{+0.05}(\omega_b), \quad (24)$$

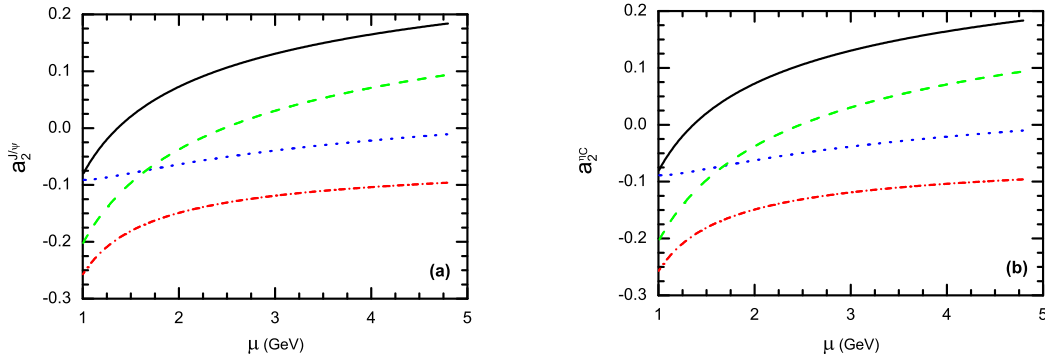


FIG. 3: Dependence of a_2 on the renormalization scale μ for (a) $B \rightarrow J/\Psi K$ and (b) $B \rightarrow \eta_c K$ decays. The solid, dashed, dotted and dash-dotted lines stand for a_2 at NLO or LO without the vertex corrections, the real part or the imaginary part of a_2 at NLO with the vertex corrections, respectively.

for $f_B = 0.19$ GeV, and $\omega_b = 0.40 \pm 0.04$ GeV. It agrees very well with that obtained in QCD sum rule calculations[28].

Now we calculate the branching ratios for those considered decay modes. With the complete decay amplitudes, we can obtain the decay width for the considered decays,

$$\Gamma(B \rightarrow M_2 K) = \frac{G_F^2 m_B^3}{32\pi} (1 - r^2) |\mathcal{M}(B \rightarrow M_2 K)|^2, \quad (25)$$

where $r = m_{J/\Psi}/m_B$ or m_{η_c}/m_B .

By using the input parameters and wave functions as given in Appendix B, we find the LO and NLO pQCD predictions (in unit of 10^{-4}) for the CP-averaged branching ratios of the four $B \rightarrow J/\Psi K$ and $\eta_c K$ decays and show them in the Table I. The predictions listed in the column one are the LO pQCD predictions by setting $\mu_0 = 1.0$ GeV. The predictions listed in the column two and three are the NLO pQCD predictions by setting $\mu_0 = 1.0$ and 1.2 GeV, respectively. The first theoretical error in these entries arises from the B meson wave function shape parameter $\omega_b = 0.40 \pm 0.04$. The second error is from the combination of the uncertainties of Gegenbauer moments $a_1^K = 0.17 \pm 0.17$ and/or $a_2^K = 0.115 \pm 0.115$. In the fifth column of Table I, as a comparison, we also cite the typical theoretical predictions obtained previously by using various approaches or models [5, 6, 9, 10].

In the last column of Table I, we list the world averages of the experimental measurements [1, 2]. One can see that the LO pQCD predictions for the branching ratios are indeed much smaller than the measured values, but the pQCD predictions with the inclusion of the vertex corrections agree well with the data for both $B \rightarrow J/\Psi K$ and $B \rightarrow \eta_c K$ decays.

Now we investigate in more detail why the vertex corrections can provide a significant enhancement. The total decay amplitudes as given in Eqs.(15) and (17) can be in general re-written in the following form

$$M = [F_C + F_P]_{Fac.} + [M_T + M_P]_{Spec.}, \quad (26)$$

TABLE I: The LO and NLO pQCD predictions of $Br(B \rightarrow J/\Psi K)$ and $Br(B \rightarrow \eta_c K)$ for $\mu_0 = 1.0$ and 1.2 GeV, respectively. For comparison, we also cite the typical theoretical predictions as given in previous literatures (in the fifth column), and the measured values [1, 2]. The unit of the branching ratios is always 10^{-4} .

Channels	LO	NLO	NLO	Others	Data
	$\mu_0 = 1.0$	$\mu_0 = 1.0$	$\mu_0 = 1.2$		
$B^0 \rightarrow J/\Psi K^0$	$2.0^{+0.2+1.9}_{-0.3-1.3}$	$13.1^{+3.6+4.2}_{-2.6-3.2}$	$9.9^{+4.0}_{-3.2}$	~ 1.0 [5]	8.71 ± 0.32
$B^+ \rightarrow J/\Psi K^+$	$2.1^{+0.3+2.1}_{-0.3-1.4}$	$14.1^{+3.8+4.4}_{-2.0-3.4}$	$10.6^{+4.3}_{-3.3}$	~ 3.3 [10]	10.07 ± 0.35
$B^0 \rightarrow \eta_c K^0$	$2.0^{+0.5+1.1}_{-0.5-1.0}$	$9.4^{+2.7+2.2}_{-2.1-2.0}$	$7.0^{+2.3}_{-2.0}$	~ 2 [9, 12]	8.9 ± 1.6
$B^+ \rightarrow \eta_c K^+$	$2.1^{+0.6+1.2}_{-0.5-1.0}$	$10.1^{+2.9+2.4}_{-2.2-2.2}$	$7.5^{+2.7}_{-2.2}$	~ 2 [10, 12]	9.1 ± 1.3

where F_C and F_P stands for the ‘‘color-suppressed’’ and the penguin part of the factorizable contribution, coming from the emission diagram Fig.1a and 1b; while M_T and M_P stands for the ‘‘Tree’’ and the penguin part of the nonfactorizable contribution, coming from the spectator diagram Fig.1c and 1d. From Eq. (15), for example, it is easy to separate the total decay amplitude $\mathcal{M}(B \rightarrow J/\Psi K)$ into the following four parts

$$F_C = F_{J/\Psi K}^{V-A} f_{J/\Psi} V_{cb}^* V_{cs} a_2;$$

$$F_P = -F_{J/\Psi K}^{V-A} f_{J/\Psi} V_{tb}^* V_{ts} (a_3 + a_5 + a_7 + a_9); \quad (27)$$

$$M_T = M_{J/\Psi K}^{V-A} V_{cb}^* V_{cs} C_2;$$

$$M_P = -M_{J/\Psi K}^{V-A} V_{tb}^* V_{ts} (C_4 - C_6 - C_8 + C_{10}) \quad (28)$$

By numerical calculations with $\mu_0 = 1.0$ GeV, we find easily the numerical values (in unit of 10^{-3}) of the individual parts and the total decay amplitude of $\mathcal{M}(B \rightarrow J/\Psi K)$ at the LO and NLO level:

$$\begin{aligned} \mathcal{M}^{LO} &= \underbrace{-1.147}_{F_C} - \underbrace{0.092}_{F_P} + \underbrace{(0.817 - i0.660)}_{M_T} + \underbrace{(0.021 - i0.036)}_{M_P}, \\ &= -0.401 - i0.696, \end{aligned} \quad (29)$$

$$\begin{aligned} \mathcal{M}^{NLO} &= \underbrace{-0.546 - i1.433}_{F_C} + \underbrace{0.004 - i0.038}_{F_P} + \underbrace{(0.775 - i0.566)}_{M_T} + \underbrace{(0.020 - i0.025)}_{M_P}, \\ &= 0.253 - i2.062, \end{aligned} \quad (30)$$

and the ratio of the square of the decay amplitude \mathcal{M}^{NLO} and \mathcal{M}^{LO} is

$$R_M(B \rightarrow J/\Psi K) = \frac{|\mathcal{M}^{NLO}|^2}{|\mathcal{M}^{LO}|^2} = 6.69. \quad (31)$$

For $B \rightarrow \eta_c K$ decay, we find the similar result: $R_M(B \rightarrow \eta_c K) = 4.8$.

From the above numerical results, it is easy to see that

- As generally expected, the penguin contributions to both the factorizable and non-factorizable parts of the total decay amplitude are always small in magnitude (less than 10%), when compared with the ‘‘T’’ and ‘‘C’’ parts.

- At the leading order, the $F_C = -1.147$ is large in size, but effectively canceled by the real part of M_T when one sums up the factorizable and nonfactorizable contributions. This strong cancelation results in a small LO pQCD prediction for the decay rates.
- At the next-to-leading order, the NLO Wilson coefficients will be used. The penguin part F_P and M_P remain small in magnitude. The variations of M_T and M_P due to the replacement of the LO Wilson coefficients by the NLO ones are also small as expected². For the “color-suppressed” F_C part, however, things become much different. Although its real part changes from -1.147 to -0.546 , becoming smaller in magnitude, but a large imaginary part $\text{Im}(F_C) = -1.433$ is produced, which leads to a large $|\mathcal{M}^{NLO}|^2$ and consequently a large NLO pQCD prediction of the branching ratios.
- At the NLO level, specifically for the case of $\mu_0 = 1.2$ GeV, the pQCD predictions for the branching ratios of the four considered decays become consistent with the data within one standard deviation. The “ $B \rightarrow (J/\Psi, \eta_c)K$ ” puzzle is therefore resolved by the inclusion of NLO contributions in the framework of the standard model.

As discussed in previous section, we choose $\mu_0 = 1.0$ GeV as the lower cut-off of the hard scale t . The explicit numerical evaluations show a moderate μ_0 -dependence of the pQCD predictions for the branching ratios, as illustrated in Fig. 4. From Table I, one can see that the consistency between the NLO pQCD predictions and the data for the case of $\mu_0 = 1.2$ GeV is better than that for the case of $\mu_0 = 1.0$ GeV. We think that the lower limit of $\mu = 1.2$ GeV is a reasonable and phenomenologically better choice than $\mu_0 = 1.0$ GeV. It is worth of noting that such a lower limit $\mu_0 = 1.2$ GeV is also coincide with the hard-collinear scale $\sqrt{\Lambda}m_b \sim 1.3$ GeV in SCET-II[29], where the perturbative calculations remain reliable, according to the general sense. For larger μ_0 , say $\mu_0 > 1.5$ GeV, too much perturbative contributions will be lost in the integration, and therefore the pQCD prediction will become further smaller, as shown in Fig. 4. We believe that a lower limit of μ_0 much larger than 1.2 GeV is unreasonable.

It is worth of mentioning that we here considered the effects of the vertex corrections only, which is available currently. Other NLO contributions coming from the Feynman diagrams as shown in Figs.5-7 in Ref. [20] are still unknown at present.

Now we turn to study the ratios of the branching ratios for some phenomenologically relevant decay modes. One advantage of the ratios is the possible cancelation of the theoretical uncertainties of individual calculations. Using the data of the measured branching

² In the evaluation of \mathcal{M}^{LO} and \mathcal{M}^{NLO} , the LO and NLO Wilson coefficients C_2 and $C_{4,6,8,10}$ will be used, respectively.

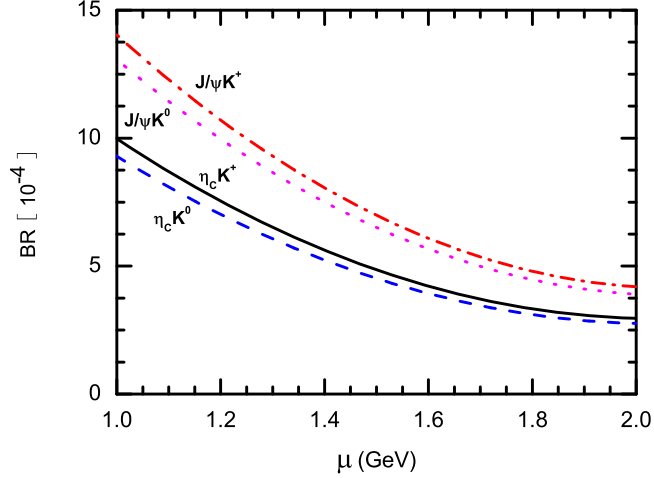


FIG. 4: The μ_0 -dependence of the NLO pQCD predictions for the branching ratios (in units of 10^{-4}) of the decay $B^+ \rightarrow J/\Psi K^+$ (dash-dotted curve), $B^0 \rightarrow J/\Psi K^0$ (dotted curve), $B^+ \rightarrow \eta_c K^+$ (solid curve) and $B^0 \rightarrow \eta_c K^0$ (dashed curve).

ratios as given in Ref.[1], the three ratios R_i^{exp} can be defined as the following

$$\begin{aligned}
 R_1^{exp} &= \frac{Br(B^+ \rightarrow \eta_c K^+)}{Br(B^+ \rightarrow J/\Psi K^+)} = 0.90 \pm 0.13, \\
 R_2^{exp} &= \frac{Br(B^0 \rightarrow \eta_c K^0)}{Br(B^0 \rightarrow J/\Psi K^0)} = 1.02 \pm 0.19, \\
 R_3^{exp} &= \frac{Br(B^0 \rightarrow \eta_c K^0)}{Br(B^- \rightarrow \eta_c K^-)} = 0.88 \pm 0.16. \quad (32)
 \end{aligned}$$

TABLE II: The ratios R_i of the pQCD predictions for the branching ratios. In the last column, the measured values of the ratios are also shown.

Ratios	LO	NLO	NLO	Data
	$\mu_0 = 1.0$	$\mu_0 = 1.0$	$\mu_0 = 1.2$	
R_1	$1.0^{+1.2}_{-0.9}$	$0.72^{+0.40}_{-0.30}$	$0.71^{+0.38}_{-0.31}$	0.90 ± 0.13
R_2	$1.0^{+1.2}_{-0.9}$	$0.72^{+0.40}_{-0.32}$	$0.93^{+0.58}_{-0.48}$	1.02 ± 0.19
R_3	$0.95^{+0.84}_{-0.74}$	$0.93^{+0.49}_{-0.41}$	$0.71^{+0.30}_{-0.26}$	0.88 ± 0.16

Based on our pQCD calculations, it is easy to find the pQCD predictions for these ratios, as listed in Table II. By comparing the pQCD predictions of the ratios and the measured ones, we can see that (a) the uncertainty of the NLO pQCD predictions is obviously smaller than that of the LO case, although we assuming the same set of input parameters ($\omega_b = 0.40 \pm 0.04$, $a_1^k = 0.17 \pm 0.17$, $a_2^k = 0.115 \pm 0.115$); (b) the predicted ratios agree with the measured ones, but the theoretical uncertainties are still large, because of our poor knowledge about the Gegenbauer moments $a_{1,2}^k$.

In short, from the above pQCD predictions for the branching ratios and the detailed phenomenological analysis, we can conclude that the pQCD approach can apply to these considered decay channels, and consequently the so-called " $B \rightarrow (J/\Psi, \eta_c)K$ " puzzle is resolved by the inclusion of the NLO vertex corrections.

B. CP-violating asymmetries

Now we turn to the evaluations of the CP-violating asymmetries of $B \rightarrow M_2 M_3$ decays in pQCD approach. For the charged B meson decays, the direct CP-violating asymmetries \mathcal{A}_{CP}^{dir} can be defined as usual. For both $B^+ \rightarrow J/\Psi K$ and $\eta_c K^+$ decays, there are no direct CP violation, since there is no weak phase appeared in their decay amplitude, as can be seen easily in Eqs. (15) and (17).

On the experiments side, the direct CP-violating parameter for the considered charged B meson decays are the following [1, 2],

$$\mathcal{A}_{CP}^{dir}(B^+ \rightarrow J/\Psi K^+) = 0.017 \pm 0.016, \quad \mathcal{A}_{CP}^{dir}(B^+ \rightarrow \eta_c K^+) = -0.16 \pm 0.08. \quad (33)$$

which are consistent with zero within 2σ level.

For the $B^0 \rightarrow M_2 M_3$ decays, because these decays are neutral B meson decays, so we should consider the effects of $B^0 - \bar{B}^0$ mixing. The direct and mixing induced CP-violating asymmetries \mathcal{A}_{CP}^{dir} and \mathcal{A}_{CP}^{mix} can be written as

$$\mathcal{A}_{CP}^{dir} = \frac{|\lambda_{CP}|^2 - 1}{1 + |\lambda_{CP}|^2}, \quad \mathcal{A}_{CP}^{mix} = \frac{2Im(\lambda_{CP})}{1 + |\lambda_{CP}|^2}, \quad (34)$$

where the CP-violating parameter λ_{CP} is

$$\lambda_{CP} = \eta_f \frac{V_{tb}^* V_{td} \langle f | H_{eff} | \bar{B}^0 \rangle}{V_{tb} V_{td}^* \langle f | H_{eff} | B^0 \rangle} = \eta_f e^{-2i\beta} \frac{\langle f | H_{eff} | \bar{B}^0 \rangle}{\langle f | H_{eff} | B^0 \rangle}, \quad (35)$$

where η_f is the CP-eigenvalue of the final states. By using the the input parameters as given in Appendix B, one found the pQCD predictions for the direct and mixing-induced CP-violating asymmetries of the considered neutral B meson decays are as follows,

$$\begin{aligned} \mathcal{A}_{CP}^{dir}(B^0 \rightarrow J/\Psi K_S^0) &= \mathcal{A}_{CP}^{dir}(B^0 \rightarrow \eta_c K_S^0) \approx 0, \\ \mathcal{A}_{CP}^{mix}(B^0 \rightarrow J/\Psi K_S^0) &= \mathcal{A}_{CP}^{mix}(B^0 \rightarrow \eta_c K_S^0) = (70.9_{-2.7}^{+2.8}) \%, \end{aligned} \quad (36)$$

where the dominant error comes from $\bar{\rho} = 0.135_{-0.016}^{+0.031}$ and $\bar{\eta} = 0.349_{-0.017}^{+0.015}$ [1]. It is easy to see that the pQCD predictions for CP -violating asymmetries agree perfectly with the experimental measurements [1, 2].

IV. CONCLUSIONS

In this paper, we calculated the branching ratios and CP-violating asymmetries of the four $B \rightarrow (J/\Psi, \eta_c)K$ decays by employing the pQCD factorization approach with the inclusion of currently available NLO vertex corrections. Besides the usual factorizable

diagrams, the non-factorizable spectator diagrams are also calculated analytically in the pQCD approach. By keeping the transverse momentum k_T in the propagators, the end-point singularity disappears in our calculation.

From our numerical calculations and phenomenological analysis, we found the following results:

- The NLO pQCD predictions for the branching ratios of the four $B \rightarrow (J/\Psi, \eta_c)K$ decays agree very well with the data:

$$\begin{aligned}
Br(B^0 \rightarrow J/\Psi K^0) &= 9.9_{-3.2}^{+4.0} \times 10^{-4}, \\
Br(B^+ \rightarrow J/\Psi K^+) &= 10.6_{-3.3}^{+4.3} \times 10^{-4}, \\
Br(B^0 \rightarrow \eta_c K^0) &= 7.0_{-2.0}^{+2.3} \times 10^{-4}, \\
Br(B^+ \rightarrow \eta_c K^+) &= 7.5_{-2.2}^{+2.7} \times 10^{-4}.
\end{aligned} \tag{37}$$

The " $B \rightarrow (J/\Psi, \eta_c)K$ " puzzle is therefore resolved by the inclusion of the vertex corrections in the pQCD approach.

- The pQCD predictions for the CP-violating asymmetries of the considered decays also agree perfectly with the data.
- From our pQCD calculations and the phenomenological analysis, we conclude that the pQCD approach can be applied to these kinds of B mesons decays.
- In this paper, only the partial NLO contributions have been taken into account. We expect that they are the dominant part of the whole NLO corrections. To achieve a complete NLO calculations in the pQCD approach, the still missing pieces should be evaluated as soon as possible.

Acknowledgments

The authors are very grateful to Hsiang-nan Li, Cai-Dian Lü and Ying Li for valuable discussions. This work is partially supported by the National Natural Science Foundation of China under Grant No.10575052, 10605012 and 10735080.

APPENDIX A: RELATED FUNCTIONS

We show here the hard function h_i 's, coming from the Fourier transformations of the function $H^{(0)}$,

$$\begin{aligned}
h_e(x_1, x_3, b_1, b_3) &= K_0 \left(\sqrt{x_1 x_3 (1-r^2)} m_B b_1 \right) \left[\theta(b_1 - b_3) K_0 \left(\sqrt{x_3 (1-r^2)} m_B b_1 \right) \right. \\
&\quad \cdot I_0 \left(\sqrt{x_3 (1-r^2)} m_B b_3 \right) + \theta(b_3 - b_1) K_0 \left(\sqrt{x_3 (1-r^2)} m_B b_3 \right) \\
&\quad \left. \cdot I_0 \left(\sqrt{x_3 (1-r^2)} m_B b_1 \right) \right] S_t(x_3),
\end{aligned} \tag{A1}$$

$$h_f(x_1, x_2, x_3, b_1, b_2) = \left\{ \theta(b_2 - b_1) I_0(m_B \sqrt{x_1 x_3 (1 - r^2)} b_1) K_0(m_B \sqrt{x_1 x_3 (1 - r^2)} b_2) + (b_1 \leftrightarrow b_2) \right\} \cdot \begin{pmatrix} K_0(m_B F_{(1)} b_2), & \text{for } F_{(1)}^2 > 0 \\ \frac{\pi i}{2} H_0^{(1)}(m_B \sqrt{|F_{(1)}^2|} b_2), & \text{for } F_{(1)}^2 < 0 \end{pmatrix}, \quad (\text{A2})$$

where J_0 is the Bessel function, K_0 and I_0 are the modified Bessel functions with $K_0(-ix) = -(\pi/2)Y_0(x) + i(\pi/2)J_0(x)$, and $F_{(j)}$'s are defined by

$$F_{(1)}^2 = (x_1 - x_2)x_3(1 - r^2) + r_c^2, \quad (\text{A3})$$

$$F_{(2)}^2 = (x_1 - x_2)x_3(1 - r^2) + r_c^2. \quad (\text{A4})$$

The threshold resummation form factor $S_t(x_i)$ can be found in Ref. [30].

The Sudakov factors used in the text are defined as

$$S_{ab}(t) = s(x_1 m_B / \sqrt{2}, b_1) + s(x_3 m_B / \sqrt{2}, b_3) + s((1 - x_3) m_B / \sqrt{2}, b_3) - \frac{1}{\beta_1} \left[\ln \frac{\ln(t/\Lambda)}{-\ln(b_1 \Lambda)} + \ln \frac{\ln(t/\Lambda)}{-\ln(b_3 \Lambda)} \right], \quad (\text{A5})$$

$$S_{cd}(t) = s(x_1 m_B / \sqrt{2}, b_1) + s(x_2 m_B / \sqrt{2}, b_2) + s((1 - x_2) m_B / \sqrt{2}, b_2) + s(x_3 m_B / \sqrt{2}, b_1) + s((1 - x_3) m_B / \sqrt{2}, b_1) - \frac{1}{\beta_1} \left[2 \ln \frac{\ln(t/\Lambda)}{-\ln(b_1 \Lambda)} + \ln \frac{\ln(t/\Lambda)}{-\ln(b_2 \Lambda)} \right], \quad (\text{A6})$$

where the function $s(q, b)$ are defined in the Appendix A of Ref. [27]. The scale t_i 's in the above equations are chosen as

$$\begin{aligned} t_e^1 &= \max(\sqrt{x_3(1 - r^2)} m_B, 1/b_1, 1/b_3), \\ t_e^2 &= \max(\sqrt{x_1(1 - r^2)} m_B, 1/b_1, 1/b_3), \\ t_f &= \max(\sqrt{x_1 x_3 (1 - r^2)} m_B, \sqrt{(x_1 - x_2)x_3(1 - r^2) + r_c^2} m_B, 1/b_1, 1/b_2), \end{aligned} \quad (\text{A7})$$

where $r = m_{M_2}/m_B (M_2 = J/\Psi, \eta_c), r_c = m_c/m_B$. The scale t_i 's are chosen as the maximum energy scale appearing in each diagram in order to kill the large logarithmic radiative corrections.

APPENDIX B: INPUT PARAMETERS AND WAVE FUNCTIONS

The masses, decay constants, QCD scale and B meson lifetime are the following

$$\begin{aligned} f_{J/\Psi} &= 0.405 \text{ GeV}, & f_K &= 0.16 \text{ GeV}, & f_{\eta_c} &= 0.42 \text{ GeV}, & m_W &= 80.41 \text{ GeV}, \\ m_{\eta_c} &= 2.98 \text{ GeV}, & m_B &= 5.2794 \text{ GeV}, & m_{J/\Psi} &= 3.097 \text{ GeV}, \\ \tau_{B^+} &= 1.643 \text{ ps}, & \tau_{B^0} &= 1.53 \text{ ps}. \end{aligned} \quad (\text{B1})$$

For the CKM matrix elements, here we adopt the Wolfenstein parametrization for the CKM matrix, and take $\lambda = 0.2257, A = 0.814, \bar{\rho} = 0.135$ and $\bar{\eta} = 0.349$ [1].

As for B meson wave function, we make use of the same parameterizations as in Ref. [27]. We adopt the model

$$\phi_B(x, b) = N_B x^2 (1-x)^2 \exp \left[-\frac{m_B^2 x^2}{2\omega_b^2} - \frac{1}{2}(\omega_b b)^2 \right], \quad (\text{B2})$$

where ω_b is a free parameter and we take $\omega_b = 0.40 \pm 0.04$ GeV in numerical calculations, and $N_B = 91.745$ is the normalization factor for $\omega_b = 0.40$.

For the vector J/ψ meson, we take the wave function as follows,

$$\Phi_{J/\Psi}(x) = \frac{1}{\sqrt{2N_c}} \left\{ m_{J/\psi} \not{x} \not{L} \phi_{J/\Psi}^L(x) + \not{x} \not{L} \not{P} \phi_{J/\Psi}^t(x) \right\}. \quad (\text{B3})$$

Here, ϕ^L denote for the twist-2 DA's, and ϕ^t for the twist-3 ones, both of them have experimental and theoretical basis[31]. x represents the momentum fraction of the charm quark inside the charmonium. The J/ψ meson asymptotic distribution amplitudes read as [31]

$$\begin{aligned} \phi_{J/\Psi}^L(x) &= 9.58 \frac{f_{J/\psi}}{2\sqrt{2N_c}} x(1-x) \left[\frac{x(1-x)}{1-2.8x(1-x)} \right]^{0.7}, \\ \phi_{J/\Psi}^t(x) &= 10.94 \frac{f_{J/\psi}}{2\sqrt{2N_c}} (1-2x)^2 \left[\frac{x(1-x)}{1-2.8x(1-x)} \right]^{0.7}. \end{aligned} \quad (\text{B4})$$

It is easy to see that both the twist-2 and twist-3 DA's vanish at the end points due to the factor $[x(1-x)]^{0.7}$.

For pseudoscalar meson η_c , the wave function is the form of

$$\Phi_{\eta_c}(x) = \frac{i}{\sqrt{2N_c}} \gamma_5 \left\{ \not{P} \phi_{\eta_c}^v + m_{\eta_c} \phi_{\eta_c}^s \right\}. \quad (\text{B5})$$

The twist-2 and twist-3 asymptotic distribution amplitudes, ϕ^v and ϕ^s , can be written as[31],

$$\begin{aligned} \phi_{\eta_c}^v(x) &= 9.58 \frac{f_{\eta_c}}{2\sqrt{2N_c}} x(1-x) \left[\frac{x(1-x)}{1-2.8x(1-x)} \right]^{0.7}, \\ \phi_{\eta_c}^s(x) &= 1.97 \frac{f_{\eta_c}}{2\sqrt{2N_c}} \left[\frac{x(1-x)}{1-2.8x(1-x)} \right]^{0.7}. \end{aligned} \quad (\text{B6})$$

The twist-2 kaon distribution amplitude ϕ_K^A , and the twist-3 ones ϕ_K^P and ϕ_K^T have

been parameterized as [32]

$$\phi_K^A(x) = \frac{f_K}{2\sqrt{2N_c}} 6x(1-x) \left[1 + a_1^K C_1^{3/2}(t) + a_2^K C_2^{3/2}(t) + a_4^K C_4^{3/2}(t) \right], \quad (\text{B7})$$

$$\phi_K^P(x) = \frac{f_K}{2\sqrt{2N_c}} \left[1 + \left(30\eta_3 - \frac{5}{2}\rho_K^2 \right) C_2^{1/2}(t) - 3 \left\{ \eta_3\omega_3 + \frac{9}{20}\rho_K^2(1 + 6a_2^K) \right\} C_4^{1/2}(t) \right], \quad (\text{B8})$$

$$\phi_K^T(x) = \frac{f_K}{2\sqrt{2N_c}} (1-2x) \left[1 + 6 \left(5\eta_3 - \frac{1}{2}\eta_3\omega_3 - \frac{7}{20}\rho_K^2 - \frac{3}{5}\rho_K^2 a_2^K \right) \times (1 - 10x + 10x^2) \right], \quad (\text{B9})$$

with $t = 2x - 1$, the Gegenbauer moments $a_1^K = 0.17$, $a_2^K = 0.115$, the parameters $\eta_3 = 0.015$, $\omega_3 = -3.0$, the mass ratio $\rho_K = (m_{u(d)} + m_s)/m_K = m_K/m_{0K}$ and the Gegenbauer polynomials $C_n^\nu(t)$,

$$\begin{aligned} C_1^{3/2}(t) &= 3t, & C_2^{1/2}(t) &= \frac{1}{2}(3t^2 - 1), & C_2^{3/2}(t) &= \frac{3}{2}(5t^2 - 1), \\ C_4^{1/2}(t) &= \frac{1}{8}(3 - 30t^2 + 35t^4), & C_4^{3/2}(t) &= \frac{15}{8}(1 - 14t^2 + 21t^4). \end{aligned} \quad (\text{B10})$$

-
- [1] C. Amsler *et al.* (Particle Data Group), Phys. Lett. B **667**, 1 (2008).
 - [2] Heavy Flavor Averaging Group, E. Barberio *et al.*, hep-ex/0808.1297v1; and online update at <http://www.slac.stanford.edu/xorg/hfag>.
 - [3] M. Gourdin, Y.Y. Keum, and X.Y. Pham, Phys. Rev. D **51**, 3510 (1995).
 - [4] H.Y. Cheng and K.C. Yang, Phys. Rev. D **59**, 092004 (1999).
 - [5] J. Chay and C. Kim, hep-ph/0009244.
 - [6] H.Y. Cheng and K.C. Yang, Phys. Rev. D **63**, 074011 (2001).
 - [7] H. Boos, J. Reuter and T. Mannel, Phys. Rev. D **70**, 036006 (2004); M. Ciuchini, M. Pierini and L. Silvestrini, Phys. Rev. Lett. **95**, 221804 (2005).
 - [8] Z.Z. Song, C. Meng, Y.J. Gao, and K.T. Chao, Phys. Rev. D **69**(2004)054009; Zhongzhi Song and Kuang-ta Chao, Phys. Lett. B **568**(2003)127-134.
 - [9] Z. Song, C. Meng, and K.T. Chao, Eur.Phys.J. C **36**(2004)365; Ce Meng, Ying-jia Gao, and Kuang-ta Chao, Communi.Theor.Phys. **48**, 885(2007);
 - [10] B. Melic, Phys. Rev. D **68**, 034004 (2003); Phys. Lett. B **591**, 91 (2004); L. Li, Z.G. Wang, and T. Huang, Phys. Rev. D **70**, 074006 (2004).
 - [11] C.-H. V. Chang and H.N. Li, Phys. Rev. D **55**, 5577 (1997); T.-W. Yeh and H.N. Li, Phys. Rev. D **56**, 1615 (1997).
 - [12] C.H. Chen and H.N. Li, Phys. Rev. D **71**, 114008 (2005).
 - [13] H.N. Li and S. Mishima, J. High Energy Phys. **03**, 009 (2007).

- [14] M. Beneke, G. Buchalla, M. Neubert, and C.T. Sachrajda, *Phys. Rev. Lett.* **83**, 1914 (1999);
- [15] H.N. Li, S. Mishima, A.I. Sanda, *Phys. Rev. D* **72**, 114005 (2005).
- [16] Y.Y. Keum, H.N. Li, and A.I. Sanda, *Phys. Rev. D* **63**, 054008 (2001); C.D. Lü, K. Ukai and M.Z. Yang, *Phys. Rev. D* **63**, 074009 (2001); C.H. Chen, Y.Y. Keum, and H.N. Li, *Phys. Rev. D* **64**, 112002 (2001); Y.Y. Keum and H.N. Li, *Phys. Rev. D* **63**, 074006 (2001).
- [17] H.N. Li, *Prog.Part.& Nucl.Phys.* **51**, 85 (2003), and reference therein.
- [18] X. Liu, H.S. Wang, Z.J. Xiao, L.B. Guo and C.D. Lü, *Phys. Rev. D* **73**, 074002 (2006); H.S. Wang, X. Liu, Z.J. Xiao, L.B. Guo and C.D. Lü, *Nucl. Phys. B* **738**, 243 (2006); Z.J. Xiao, X.F. Chen and D.Q. Guo, *Eur.Phys.J. C* **50**, 363 (2007); Z.J. Xiao, D.Q. Guo and X.F. Chen, *Phys. Rev. D* **75**, 014018 (2007); Z.J. Xiao, X. Liu and H.S. Wang, *Phys. Rev. D* **75**, 034017 (2007).
- [19] A. Ali, G. Kramer, Y. Li, C.D. Lü, Y.L. Shen, W. Wang, and Y.M. Wang, *Phys. Rev. D* **76**, 074018 (2007).
- [20] Z.J. Xiao, Z.Q. Zhang, X. Liu and L.B. Guo, *Phys. Rev. D* **78**, 114001 (2008).
- [21] Z.Q. Zhang and Z.J. Xiao, *Eur.Phys.J. C* **59** (2009) in press, arXiv:0807.2022[hep-ph]; Z.Q. Zhang and Z.J. Xiao, arXiv:0807.2024[hep-ph]; J. Liu, R. Zhou and Z.J. Xiao, arXiv:0812.2132[hep-ph].
- [22] Y. Li and C.D. Lü, *J. Phys. G* **29**, 2115 (2003); *High Energy & Nucl.Phys.* **27**, 1061 (2003); Y. Li, C.D. Lü, and Z.J. Xiao, *J. Phys. G* **31**, 273 (2005); Y. Li, C.D. Lü, and C.F. Qiao, *Phys. Rev. D* **73**, 094006 (2006).
- [23] Z.J. Xiao, X. Liu, *Int.J.Mod.Phys. A* **23**, 3246 (2008);
- [24] H.N. Li, *Phys. Rev. D* **66**, 094010 (2002).
- [25] H.N. Li and B. Tseng, *Phys. Rev. D* **57**, 443 (1998).
- [26] G. Buchalla, A.J. Buras, and M.E. Lautenbacher, *Rev. Mod. Phys.* **68**, 1125 (1996).
- [27] C.-D. Lü, K. Ukai and M.Z. Yang, *Phys. Rev. D* **63**, 074009 (2001).
- [28] G. Duplancić and B. Melić, *Phys. Rev. D* **78**(2008)054015.
- [29] M. Beneke, *Nucl.Phys.B(Proc.Suppl.)* **170**, 57 (2007).
- [30] T. Kurimoto, H.N. Li, and A.I. Sanda, *Phys. Rev. D* **65**, 014007 (2001); *Phys. Rev. D* **67**, 054028 (2003).
- [31] A.E. Bondar and V.L. Chernyak, *Phys. Lett. B* **612**, 215(2005).
- [32] P. Ball, *J. High Energy Phys.* 9809, 005 (1998); P. Ball, *J. High Energy Phys.* 9901, 010 (1999); P. Ball and R. Zwicky, *Phys. Rev. D* **71**, 014015 (2005); P. Ball, V.M. Braun, and A. Lenz, *J. High Energy Phys.* **0605**, 004 (2006).